AIAA-2005-0208

ACOUSTIC SIMULATION OF HOT COAXIAL JETS USING COLD HELIUM-AIR MIXTURE JETS

Dimitri Papamoschou*
University of California, Irvine, Irvine, California 92697-3975

This work examines the ability of small-scale, helium-air-mixture, coaxial jets to capture the acoustics of large-scale hot jets representing the exhaust of separate-flow turbofan engines. Experiments at University of California, Irvine (UCI) employed a one-eighth-scale model of a separate-flow nozzle being used at the Nozzle Acoustic Test Rig (NATR) of NASA Glenn Research Center. Comparisons were conducted for two set points using the following methods: matching velocity and density, and matching velocity and Mach number. For both methods, the UCI data compare very well with the NATR data in all measures of noise: spectral shapes, spectral levels, and overall sound pressure levels. The method of matching velocity and Mach number gives slightly better agreement in the spectral shapes at angles close to the jet axis, and in the overall sound pressure levels. The overall agreement between the UCI and NATR data is within one decibel.

Nomenclature

a	=	mean speed of sound
B	=	bypass ratio
c_{He}	=	helium mass fraction
D	=	nozzle diameter
M	=	Mach number
NPR	=	nozzle pressure ratio
p	=	pressure
U	=	velocity
θ	=	polar angle relative to jet axis
ϕ	=	azimuth angle
ρ	=	density

Subscripts

a	=	ambient
f	=	fan
p	=	primary (core) stream
s	=	secondary (bypass) stream
0	=	total (stagnation)

*Professor, Associate Fellow AIAA

Introduction

Jet aeroacoustics remains one of the most challenging fields of continuum mechanics. Despite substantial progress in the understanding and modeling of jet noise, computation from first principles remains inadequate for predicting sound emission from practical jets. Therefore, the only way to obtain reliable data is via experiments. Given the wealth of variables influencing sound emission (velocity, Mach number, density, bypass ratio, nozzle shape, etc.), experiments need to cover a large parameter space in order to produce results that are meaningful to aircraft noise prediction and control. It is easy to see how this can becomes a very expensive process.

Jet aeroacoustic facilities in the United States that test nozzles with realistic geometry and realistic flow conditions are about $1/10^{\mathrm{th}}$ the scale of the actual engine. They exist at NASA Centers and in industry. These facilities have been instrumental in the advancement of knowledge on jet noise and the investigation of novel concepts for noise suppression, several of which have benefited the aerospace industry [1]. There is no substitute for their capability and scientific value. However, their operation is very expensive and investigations can be lengthy.

University facilities tend to be an order of magnitude smaller, about $1/100^{\mathrm{th}}$ to $1/50^{\mathrm{th}}$ scale. The majority of university experiments have investigated single-stream jets composed of cold air and issuing from simple nozzles. Few rigs are equipped to run hot, fewer are dual-stream, and even fewer use nozzles representative of the nozzle of a turbofan engine. It should be realized that a hot jet experiment in a university setting is an expensive proposition fraught with safety and environmental concerns. While it is doable, one sacrifices the flexibility, low cost, and low risk of a cold experiment.

A method to match approximately the conditions of a hot jet, while still running "cold", is to replace the air by a gas, or a gas mixture, with lower molecular weight. Helium is a prime candidate because of its very low molecular weight and because it is non-toxic and non-combustible. The use of helium-air mixture jets for the study of jet aeroacoustics was pioneered by Chan and Westley [2] and subsequently was used by Kinzie and McLaughlin [3] and Papamoschou [5]. In comparing single-stream jets composed of helium-air mixtures with hot air jets, Kinzie and McLaughlin demonstrated excellent agreement in the acoustics and mean flow behavior. The aeroacoustics program at UCI has used helium-air mixtures for the simulation of heated single- and dual-stream jets.

A question that invariably arises is the following: how reliable are very-small-scale, helium-air jets in duplicating the acoustics of *realistic* full-scale, heated jets? Realistic here means dual-stream with nozzle geometry representative of that in a turbofan engine. It is very important to note that all commercial (and most of the military) engine exhausts are dual-stream. Even in the case of internal mixers, the exhaust is never uniform enough to be characterized as single-stream.

This study addresses the above question by surveying the acoustics of very-small-scale, helium-air mixture, coaxial jets issuing from a nozzle with realistic and comparing them to the acoustics of equivalent heated jets tested at the Nozzle Acoustic Test Rig (NATR) of NASA Glenn Research Center. The NATR nozzle is eight times the size of the UCI nozzle. The paper gives a short introduction on the use of helium-air mixture, describes the UCI and NATR nozzles, and compares the data from the two facilities.

Helium-Air Mixtures

An excellent treatment on the use of helium-air mixtures for jet aeroacoustics can be found in Doty and McLaughlin [4]. Here we present a brief overview on the ability of helium-air mixtures to capture the acoustics and fluid mechanics of hot jets. In attempting to recreate a hot jet, one would like to match the following parameters at the nozzle exit:

Mach number. This is a function of the nozzle pressure ratio NPR=p_0/p_a and, in the case of imperfectly expanded flow, the nozzle area ratio. Assuming perfectly expanded flow,

$$M = \sqrt{\frac{2}{\gamma - 1}\left[\mathrm{NPR}^{(\gamma-1)/\gamma} - 1\right]} \qquad (1)$$

Velocity

$$U = Ma = M\sqrt{\gamma R T} \qquad (2)$$

Density

$$\rho = \frac{p_a}{RT} \qquad (3)$$

Lighthill's acoustic analogy has shown the profound effect that jet velocity has on sound emission. For jets with speeds not much higher than the ambient speed of sound, a dimensional analysis of Lighthill's equation shows that the acoustic intensity scales as U^8, a trend corroborated by experimental data [6]. It is therefore the premise of this study that the velocity U must be matched. Assuming for a moment that the Mach number M is also matched, the cold mixture jet achieves the same velocity as a hot air jet by increasing γR in Eq. 2.

Helium causes a small complication in that it is a monatomic gas, thus has a specific heat ratio $\gamma = 5/3 = 1.6667$ which is different from the diatomic value $\gamma = 7/5 = 1.4$ for air. A helium-air mixture therefore has $1.4 < \gamma < 1.6667$. The practical impact is that we can match exactly only two of the three aforementioned parameters; the remaining parameter will be matched only approximately, within a few percent. In this investigation we will compare two approaches: matching velocity *and* density versus matching velocity *and* Mach number.

Experimental Details of UCI Facility

The nozzle of the UCI experiments is a scaled-down version of the baseline separate-flow nozzle used in the NATR tests, henceforth called the 3BB nozzle. The radial coordinates of the 3BB nozzle were obtained from NASA Glenn and were scaled down by a factor of about eight to fit within the flow capacity of the UCI lab. Stereolithography files were created and the nozzle components were rapid-prototyped from plastic (epoxy resin) material. Because plastic cannot be machined to very small thickness, the relative thickness of the UCI nozzle at the trailing edge is larger than that of the NATR nozzle. Figure 1 shows the combined stereolithography file of the three elements of the UCI nozzle: fan nozzle, core nozzle, and plug. Figure 2 plots the coordinates of the NATR and UCI nozzles. The fan exit diameters D_f of the UCI and NATR nozzles are 1.22 in. and 9.69 in., respectively. In other words, the NATR nozzle is 7.94 times larger than the UCI nozzle.

The scaled-down 3BB nozzle was tested in the Jet Aeroacoustics Facility at UCI, shown in Figs. 3 and 4. The facility supplies mixtures of helium and air to the primary (core) and secondary (bypass) nozzles. The helium mass fraction c_{He} and the total pressure p_0 of each mixture are determined by the desired exit velocity and Mach number. The nozzle size sets the individual mass flow rates of air and helium. Corresponding to the mass flow rate of air is the total pressure of the air flow alone, $p_{0_{\mathrm{air}}}$. The helium mass fraction is set by first running air alone through the nozzle to match $p_{0_{\mathrm{air}}}$, then adding helium to match p_0. This is the same procedure used by Doty and McLaughlin [4].

The UCI experiments tried to match the conditions of two NATR static tests with fully-mixed equivalent jet velocities $U_{\mathrm{mix}} = 1162$ ft/s and 1202 ft/s. The NATR tests are described in Janardan et al. [9]. The matching methods were the two discussed earlier, i.e., matching velocity and density; and matching velocity and Mach number. For each set point and matching method, the total pressures were held to within 0.5% of the target values, resulting in errors of 0.4% in the velocity and 0.2% in the Mach number. The Reynolds number of the jet, based on fan diameter, was 0.6×10^6 for UCI and 4.8×10^6 for NATR.

Noise measurements were conducted inside an anechoic chamber using a one-eighth inch condenser microphone (Brüel & Kjær 4138) with frequency response of 140 kHz. The microphone was mounted on a pivot arm and traced a circular arc centered at the jet exit with radius of $r = 38$ in., or $r/D_f = 31.1$. The polar angle θ ranged from 25° to 130° relative to the jet axis. The microphone was sampled at 400 kHz by a fast analog-to-digital board (National Instruments PCI-6070E) installed in a Pentium 4 computer. Each recording consisted of 54280 samples (135 ms), corresponding to the passage of about 10,000 eddies the size of the inner-jet diameter. The signal was high-pass filtered at 500 Hz by a Butterworth filter to remove spurious low-frequency noise. The narrowband power spectrum of the microphone voltage was computed using a 2048-point Fast Fourier Transform, which provided a spectral resolution of 195 Hz. Using the microphone's sensitivity of 1 mV/Pa and accounting for the amplifier gain setting, the voltage power spectrum was converted to the power spectrum of p'/p_{ref}, where p' is the pressure fluctuation and $p_{ref} = 20\ \mu$Pa is the commonly used reference pressure. Converted to decibels, this becomes the spectrum of the sound pressure level, $\mathrm{SPL}_{\mathrm{raw}}(f)$, where f is the measured frequency. This spectrum must undergo several corrections before accurate data can be extracted. The corrected spectrum is given by

$$\mathrm{SPL}(f) = \mathrm{SPL}_{\mathrm{raw}}(f) - C_{\mathrm{fr}}(f) - C_{\mathrm{ff}}(f) + \alpha(f)r \quad (4)$$

where C_{fr} and C_{ff} are the corrections for the actuator response and free-field response, respectively; they are based on data provided by the manufacturer of the microphone. α is the atmospheric absorption coefficient (dB/m), computed using the formulas proposed by Bass et al. [8] for the measured values of relative humidity and temperature of the ambient air. The overall sound pressure level was obtained by integrating the corrected spectrum:

$$\mathrm{OASPL} = 10 \log_{10} \int_0^{f_{\mathrm{upper}}} 10^{0.1\mathrm{SPL}(f)} df \quad (5)$$

where the upper limit is the highest frequency that can be resolved, in this case 140 kHz.

Procedure for Comparing with NATR Data

The Nozzle Acoustic Test Rig has been described in earlier publications [9]. Here we discuss the method of comparing the UCI results with the NATR results. The NATR spectra are presented as lossless, 1/3-octave spectra corresponding to the actual frequencies measured in that facility. They are referenced to a 12-in. arc centered at the nozzle exit, that is, $r/D_f = 1.24$.

The UCI data were scaled to the conditions of the NATR data using the following procedure:

1. The UCI frequencies were divided by the scale factor 7.94. The highest resolvable frequency was 140 kHz/7.94 = 17.6 kHz.

2. The scaled-up narrowband UCI spectra were converted into 1/3-octave spectra.

3. The UCI 1/3-octave spectra were incremented by the distance factor

$$20\log_{10}\left[\frac{(r/D_f)_{UCI}}{(r/D_f)_{NATR}}\right]$$

$$= \ 20\log_{10}(31.1/1.24) \ = \ 28.0 \text{ dB}$$

Comparisons of Spectra

Spectra were plotted up to the maximum resolvable frequency of the UCI data, namely 17600 Hz. They will be shown for a variety of polar angles. We compare the UCI and NATR spectra for the two set points (U_{mix} = 1162 ft/s and 1202 ft/s) using the method of matching velocity and density, and the method of matching velocity and Mach number. Table 1 shows the NATR conditions of the first set point and the corresponding UCI conditions using the aforementioned matching methods. Table 2 shows the analogous information for the second set point. The UCI conditions shown in the tables represent average conditions over the coverage of all the polar angles for each case. Slight departures from the target values are due to small errors in setting the total pressures, discussed earlier.

First we examine the method of comparing at equal velocity and density. Spectra at selected polar angles are shown in Figures 5 and 6 for set points U_{mix} = 1162 ft/s and 1202 ft/s, respectively. For both set points, the UCI spectra agree very well with the NATR spectra, except at very small angles ($\theta = 20°$) where small discrepancies are noted. Next we compare at equal velocity and Mach number. Spectra at selected polar angles are shown in Figures 7 and 8 for set points U_{mix} = 1162 ft/s and 1202 ft/s, respectively. We note excellent agreement for all the polar angles.

Comparisons of Overall Sound Pressure Levels

Figure 9 plots the OASPL directivities of the NATR and UCI data using the method of matching velocity and density. While the overall agreement is very good, the UCI data slightly underpredict OASPL at the larger polar angles. Comparing at same velocity and Mach number, Fig. 10, produces even better agreement and the underprediction at the large angles becomes very small.

The quality of agreement between the UCI and NATR data can be expressed in terms of the root mean square deviation

$$\Delta\text{OASPL} = \sqrt{\frac{1}{N}\sum_{k=1}^{N}(\text{OASPL}_{\text{UCI, k}} - \text{OASPL}_{\text{NATR, k}})^2}$$

where the summation is over the fourteen polar angles measured in the UCI experiment. For the method of matching velocity and density, the deviation is 1.3 dB and 1.4 dB for U_{mix} = 1162 ft/s and 1202 ft/s, respectively. When matching velocity and Mach number, the corresponding deviations are 1.2 dB and 1.0 dB.

Conclusions

The acoustics of large-scale, hot, coaxial jets are duplicated very accurately by equivalent small-scale, cold, helium-air mixture jets. There is very good agreement in the spectral shapes, spectral levels, and overall sound pressure levels. Matching velocity and Mach number gives slightly superior agreement than matching velocity and density. The helium-air mixture jets allow for flexible and relatively inexpensive parametric studies of exhaust flows of practical significance to aircraft engines. The cold flow simplifies operation and enables use of plastic rapid-prototyped nozzles which are cheap to manufacture. The physics of sound emission can be investigated at a cost dramatically lower than in large heated rigs.

It is important, however, to point out some limitations of very small jet facilities. The spatial resolution of flow field measurements cannot be as good as in large facilities. There are limits on the frequency resolution of the acoustic measurements (see "Experimental Details" section), although the impact of these limits on perceived noise level is small [10].

The ability to accurately manufacture nozzle modifications such as chevrons, deflectors, etc., is impeded by the small size of the nozzle. Because of the smaller Reynolds number, the relative boundary-layer thickness is greater than in large-scale facilities, which could affect the performance of subtle nozzle trailing edge modifications.

In other words, the small-scale helium-air tests will not replace the value of large-scale hot tests, especially when it comes to nozzles with modifications. The ultimate acoustic benefit of new nozzle concepts should be assessed in a large facility. Helium-air jets can provide valuable guidance for understanding the physics, exploring new configurations, and optimizing noise-reduction concepts.

Acknowledgments

The support by NASA Glenn Research Center is gratefully acknowledged (Grant NAG-3-2345 monitored by Drs. Khairul B. Zaman and James Bridges). Dr. Bridges is especially thanked for providing us with the NATR nozzle coordinates and acoustic data.

References

[1] Saiyed, N.H., Mikkelsen, K.L., and Bridges, J.E., "Acoustics and Thrust of Separate-Flow High-Bypass-Ratio Engines," *AIAA Journal*, Vol. 41, No. 3, 2003, pp. 372-378.

[2] Chan, Y.Y. and Westley, R. "Directional Acoustic Radiation Generated by Spatial Jet Instability," *CASI Transactions,* Vol. 6, 1973, pp. 36-41.

[3] Kinzie, K.W. and McLaughlin, D.K., "Measurements of Supersonic Helium/Air Mixture Jets," *AIAA Journal,* Vol. 37, No. 11, 1999, pp. 1363-1369.

[4] Doty, M.J. and McLaughlin, D.K., "Acoustic and Mean Flow Measurements of High-Speed, Helium-Air Jets," *International Journal of Aeroacoustics,* Vol. 2, No. 3 & 4, 2003, pp.293-333.

[5] Papamoschou, D., "Mach Wave Elimination in Supersonic Jets," —it AIAA Journal, Vol. 35, No.10, 1997, pp. 1604-1611

[6] Dowling, A. and Ffowcs-Williams, J. "Sound and Sources of Sound", Ellis Horwood, 1983, pp.157-163.

[7] Papamoschou, D. and Debiasi, M. "Noise Measurements in Supersonic Jets Treated with the Mach Wave Elimination Method," *AIAA Journal*, Vol. 37, No. 2, 1999, pp. 154-160.

[8] Bass, H.E., Sutherland, L.C., Blackstock, D.T., and Hester, D.M., "Atmospheric Absorption of Sound: Further Developments, " *Journal of the Acoustical Society of America,* Vol. 97, No. 1, 1995, pp. 680-683.

[9] Janardan, B.A., Hoff, G.E., Barter, J.W., Martens, S., Gliebe, P.R., Mengle, V., and Dalton, W.N., "AST Critical Propulsion and Noise Reduction Technologies for Future Commercial Subsonic Engines Separate-Flow Exhaust System Noise Reduction Concept Evaluation," NASA CR 2000-210039.

[10] Papamoschou, D. and Debiasi, M., "Conceptual Development of Quiet Turbofan Engines for Supersonic Aircraft," *AIAA Journal of Propulsion and Power,*, Vol. 18, No.2, 2003, pp. 161-169.

Table 1 Exit conditions for $U_{\mathrm{mix}} = 1162$ ft/s

Quantity	NATR	UCI[a]	UCI[b]
NPR_p	1.688	1.690	1.765
M_p	0.898	0.857	0.898
U_p (ft/s)	1586	1590	1593
ρ_p/ρ_a	0.408	0.409	0.445
$c_{\mathrm{He,p}}$	-	0.305	0.281
γ_p	1.400	1.575	1.568
NPR_s	1.842	1.826	1.850
M_s	0.976	0.962	0.975
U_s (ft/s)	1077	1073	1075
ρ_s/ρ_a	1.044	1.043	1.061
$c_{\mathrm{He,s}}$	-	0.027	0.023
γ_s	1.400	1.429	1.420
B	4.98	5.15	4.88

[a] Matching velocity and density
[b] Matching velocity and Mach number

Table 2 Exit conditions for $U_{\mathrm{mix}} = 1202$ ft/s

Quantity	NATR	UCI[a]	UCI[b]
NPR_p	1.793	1.780	1.884
M_p	0.953	0.898	0.952
U_p (ft/s)	1692	1685	1692
ρ_p/ρ_a	0.403	0.408	0.452
$c_{\mathrm{He,p}}$	-	0.321	0.291
γ_p	1.400	1.581	1.571
NPR_s	1.898	1.890	1.905
M_s	1.002	0.990	1.002
U_s (ft/s)	1102	1102	1102
ρ_s/ρ_a	1.051	1.048	1.072
$c_{\mathrm{He,s}}$	-	0.028	0.025
γ_s	1.40	1.430	1.427
B	4.85	5.14	4.74

[a] Matching velocity and density
[b] Matching velocity and Mach number

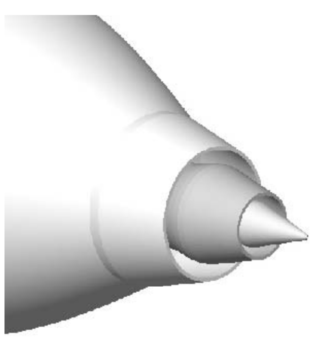

Fig.1 Stereolithography file of UCI nozzle.

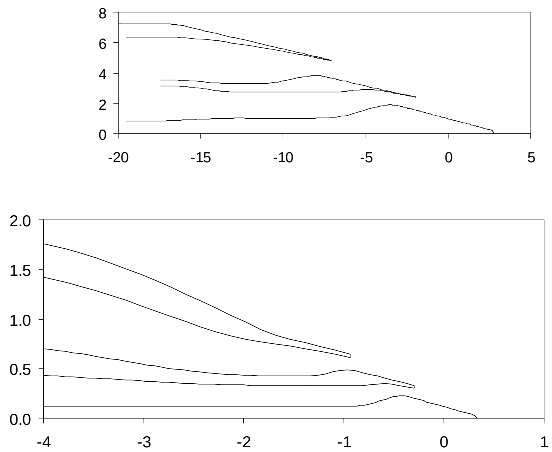

Fig.2 Radial coordinates of NATR and UCI nozzles. Units are inches.

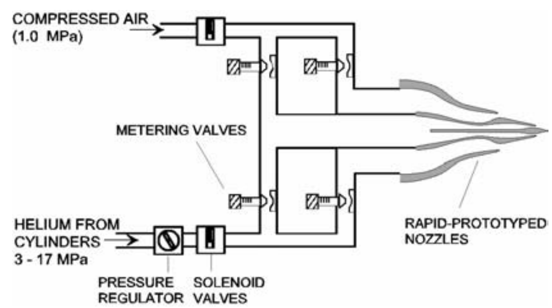

Fig.3 UCI dual-stream jet apparatus.

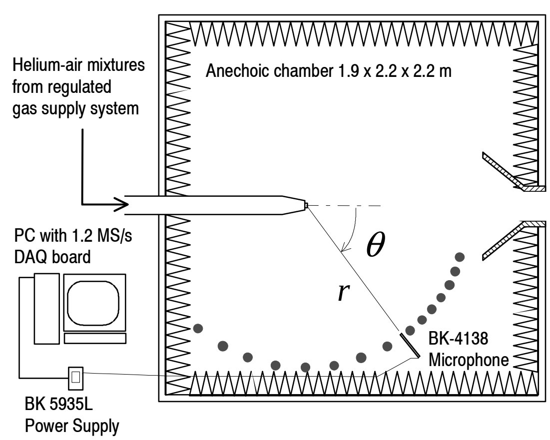

Fig.4 UCI Jet aeroacoustic facility.

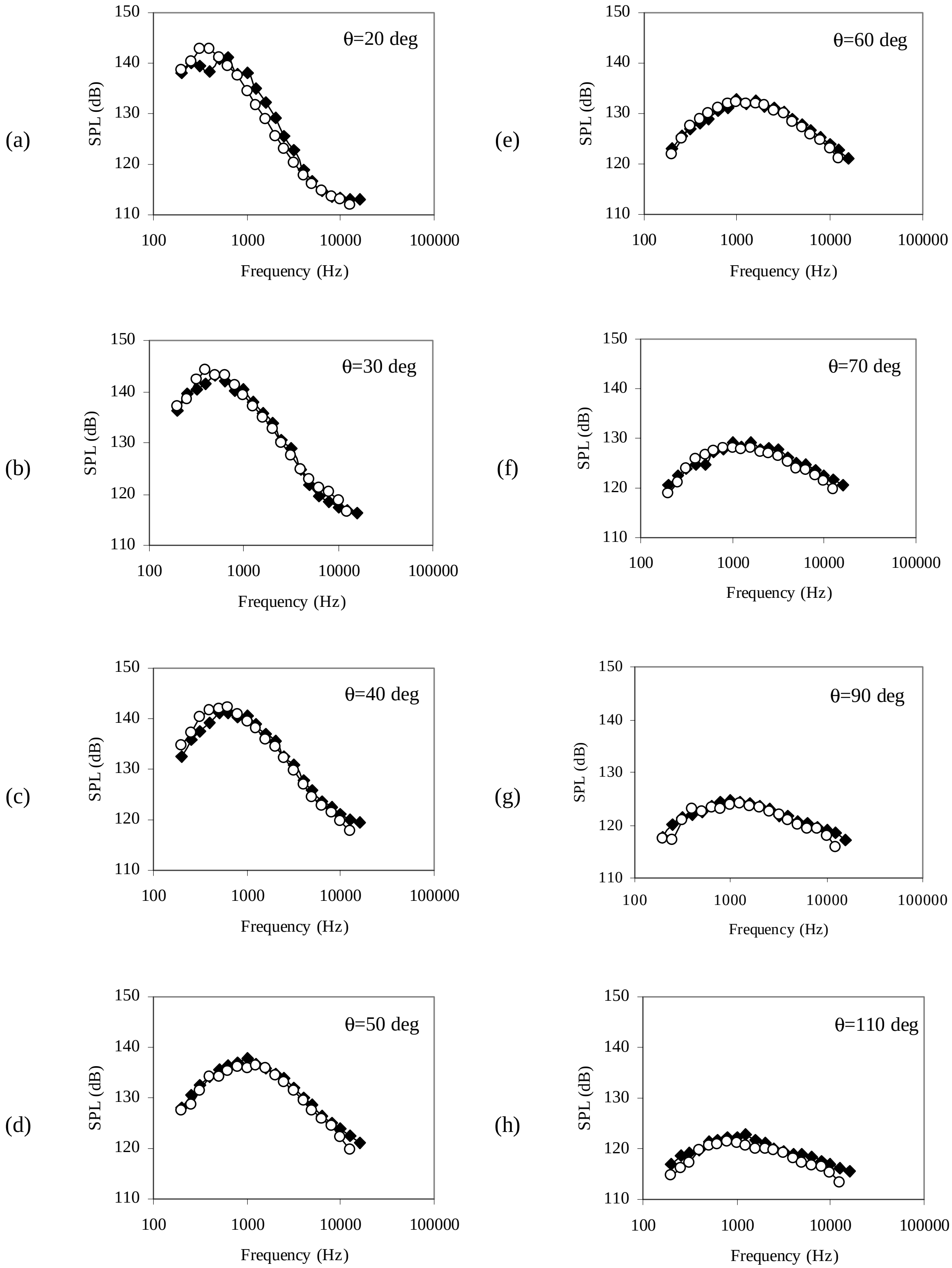

Fig.5 Spectral comparisons for $U_{\mathrm{mix}} = 1162$ ft/s, using the method of matching velocity and density. Solid symbols: NATR spectra; open symbols: UCI spectra. (a) $\theta = 20°$; **(b)** $\theta = 30°$; **(c)** $\theta = 40°$; **(d)** $\theta = 50°$; **(e)** $\theta = 60°$; **(f)** $\theta = 70°$; **(g)** $\theta = 90°$; **(h)** $\theta = 110°$.

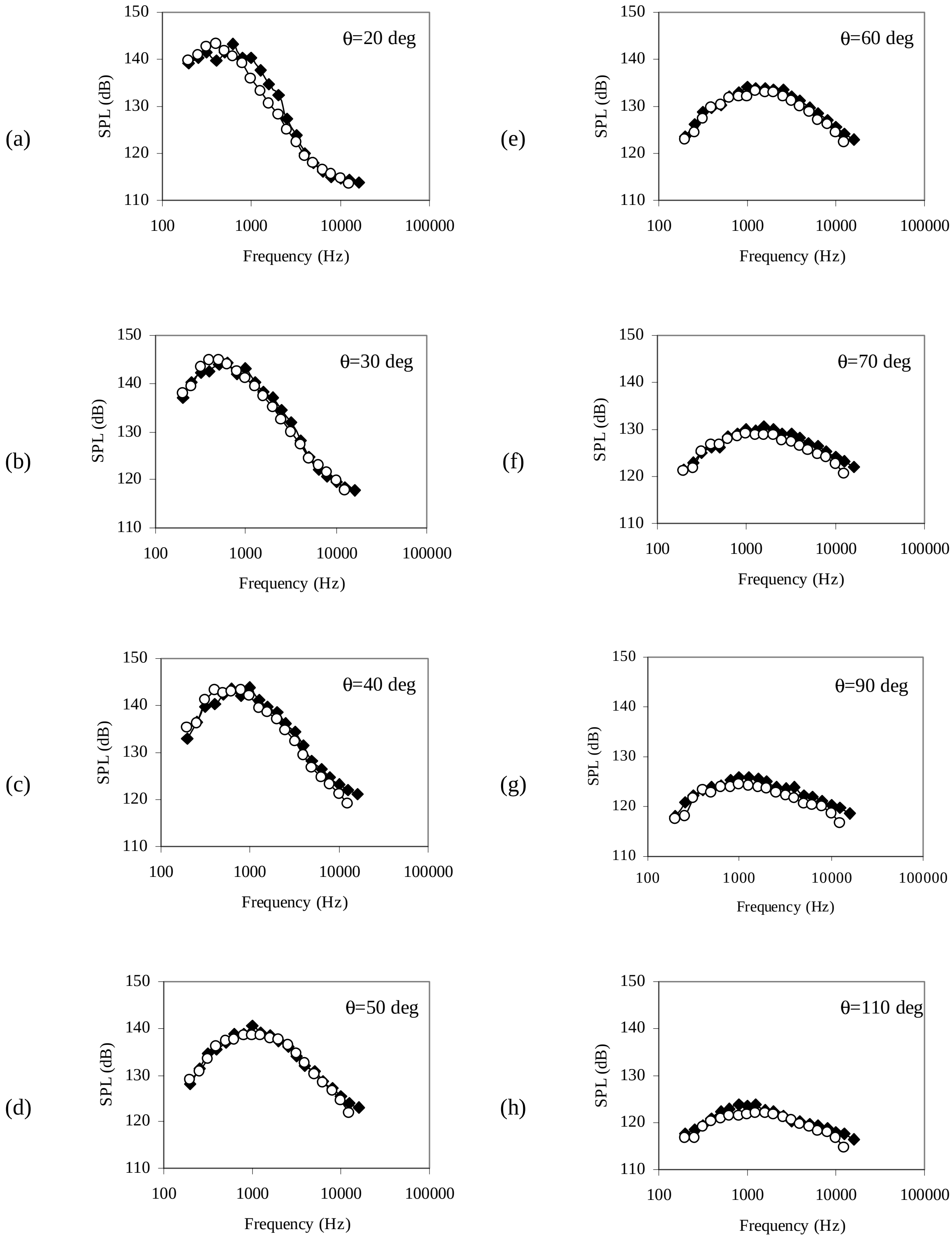

Fig.6 Spectral comparisons for $U_{\text{mix}} = 1202$ ft/s, using the method of matching velocity and density. Solid symbols: NATR spectra; open symbols: UCI spectra. (a) $\theta = 20°$; **(b)** $\theta = 30°$; **(c)** $\theta = 40°$; **(d)** $\theta = 50°$; **(e)** $\theta = 60°$; **(f)** $\theta = 70°$; **(g)** $\theta = 90°$; **(h)** $\theta = 110°$.

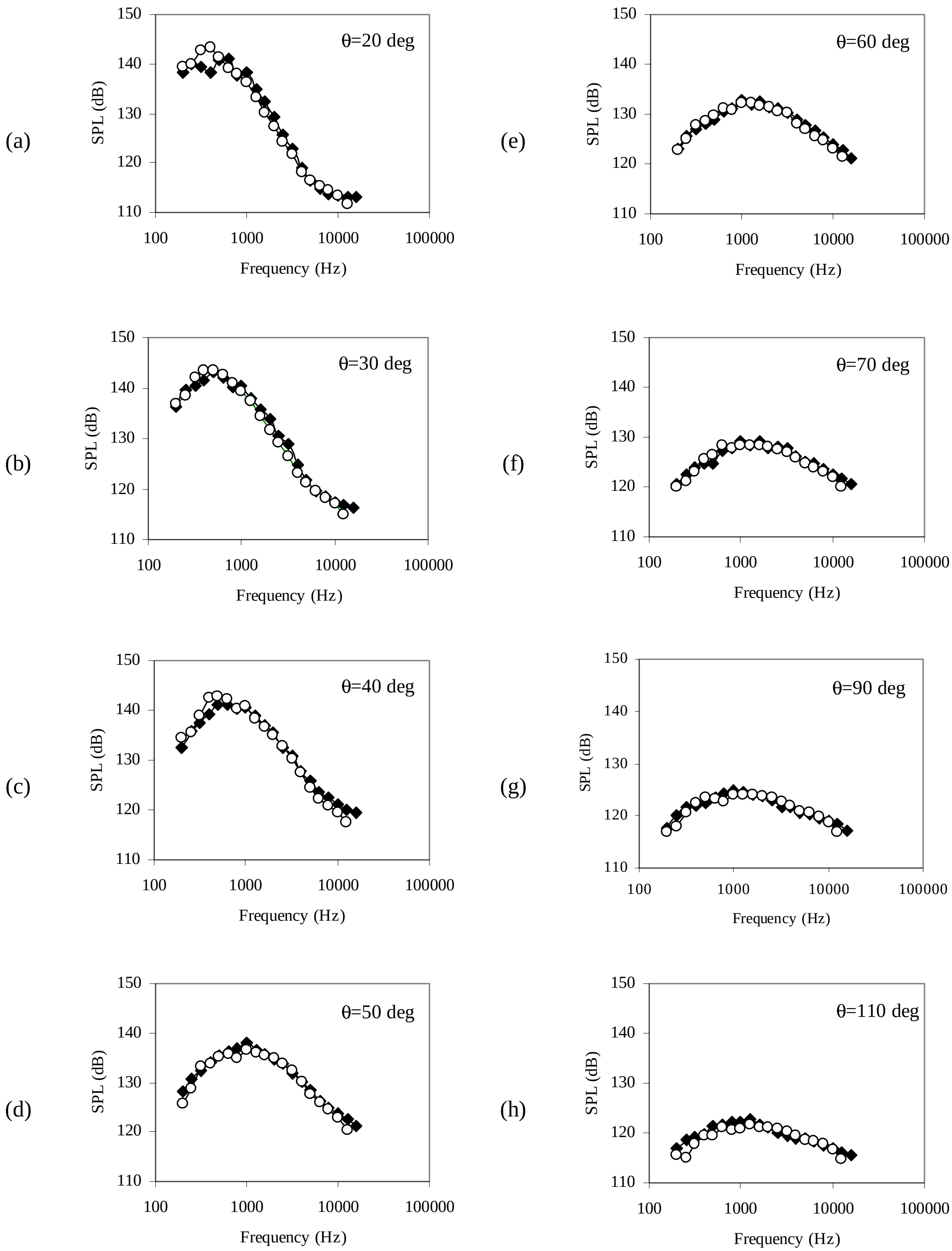

Fig.7 Spectral comparisons for $U_{\mathrm{mix}} = 1162$ ft/s, using the method of matching velocity and Mach number. Solid symbols: NATR spectra; open symbols: UCI spectra. (a) $\theta = 20°$; **(b)** $\theta = 30°$; **(c)** $\theta = 40°$; **(d)** $\theta = 50°$; **(e)** $\theta = 60°$; **(f)** $\theta = 70°$; **(g)** $\theta = 90°$; **(h)** $\theta = 110°$.

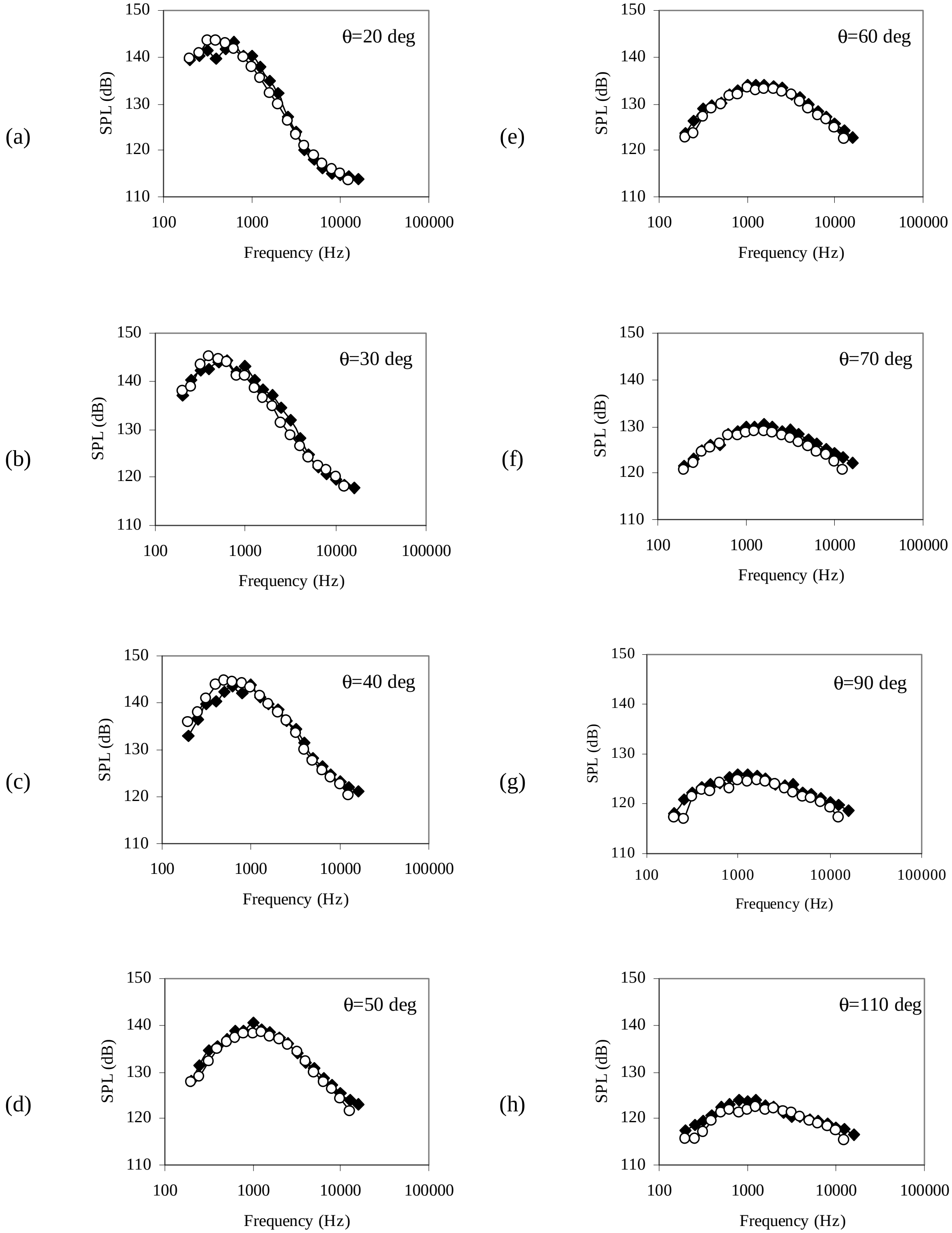

Fig.8 Spectral comparisons for $U_{\text{mix}} = 1202$ ft/s, using the method of matching velocity and Mach number. Solid symbols: NATR spectra. Open symbols: UCI spectra. (a) $\theta = 20°$; (b) $\theta = 30°$; (c) $\theta = 40°$; (d) $\theta = 50°$; (e) $\theta = 60°$; (f) $\theta = 70°$; (g) $\theta = 90°$; (h) $\theta = 110°$.

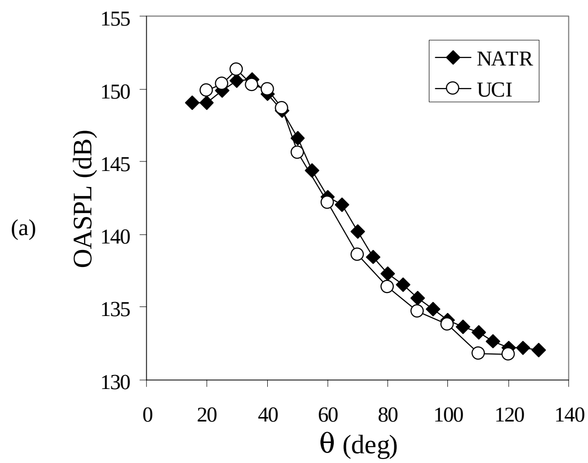

Fig.9 Comparison of OASPL using the method of matching velocity and density. (a) $U_{\mathrm{mix}} = 1162$ **ft/s; (b)** $U_{\mathrm{mix}} = 1202$ **ft/s.**

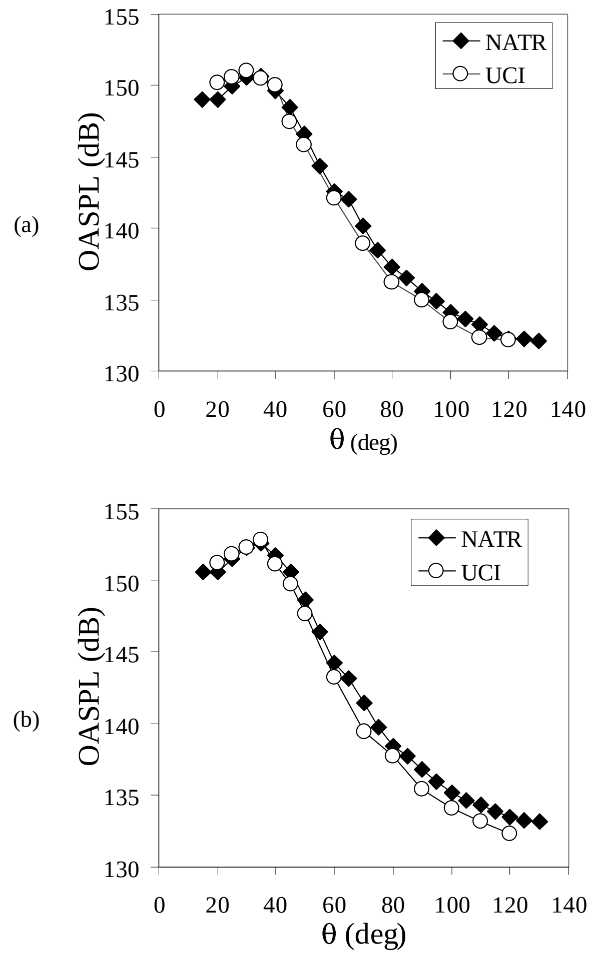

Fig.10 Comparison of OASPL using the method of matching velocity and Mach number. (a) $U_{\mathrm{mix}} = 1162$ **ft/s; (b)** $U_{\mathrm{mix}} =$ 1202 **ft/s.**